AFGC-ACI-*fib*-RILEM Int. Symposium on Ultra-High Performance Fibre-Reinforced Concrete, **UHPFRC 2017** – October 2-4, 2017, Montpellier, France

IDENTIFICATION OF THE TENSILE LAW OF UHPFRC MATERIALS FROM BENDING TESTS BY MEANS OF DIGITAL IMAGE CORRELATION

Youri Duhamel-Labrecque (1), Luca Sorelli (1), Julien Réthoré (2), Florent Baby (3), François Toutlemonde (3) and Sébastien Bernardi (4)

(1) Department of Civil Engineering, Université Laval, Quebec, G1V0A6, Canada
(2) École Centrale de Nantes, Université de Nantes, France
(3) Université Paris-Est/IFSTTAR, France
(4) Ductal®, LafargeHolcim, Paris, France

Abstract

The use of Ultra High Performance Fibre Reinforced Concrete (UHPFRC) requires the use of the tensile law which is commonly identified by inverse analysis from bending tests. The aim of this work is to foster the identification of the UHPFRC tensile law by means of Digital Image Correlation (DIC) analysis in order to account the distribution of multiple cracks, the asymmetric position of the localized crack and the unloading of the micro-cracked parts. A series of unnotched UHPFRC beams with fibre volume content of 1% and 2% were tested under 4 point bending tests (4PBT). The relationships moment-curvature M-X and moment-rotation M-θ were identified by best-fitting the deflection and rotation over the beam length at all time steps. By considering the rotation compatibility mechanisms, the characteristic length L_{ch} was also estimated. Finally, the UHPC tensile law is estimated from the M-X relation. In agreement with previous methods, the proposed method was able to systematically distinguish strain hardening and softening UHPFRC.

Résumé

L'emploi des bétons fibrés à ultra-hautes performances (BFUP) nécessite d'utiliser une loi de comportement en traction qui est généralement déduite par analyse inverse d'essais de flexion. Le but de ce travail est de favoriser l'identification de cette loi en utilisant l'analyse d'images, afin de tenir compte de la multi-fissuration, de la dissymétrie introduite par la localisation de la fissure principale et du déchargement des zones micro-fissurées. Une série de poutres en BFUP non entaillées avec un taux de fibres de 1 ou 2 % a fait l'objet d'essais de flexion 4 points. Les relations moment-courbure et moment-rotation ont été identifiées par approximation de la déflexion et de la rotation sur la longueur de la poutre à chaque pas de chargement. En considérant la compatibilité des rotations, la longueur caractéristique L_{ch} a également été évaluée. Enfin, la loi de comportement en traction du BFUP a été déduite de la relation moment-courbure. En accord avec les méthodes préexistantes, la méthode proposée a permis de distinguer systématiquement les BFUP écrouissants des BFUP adoucissants.

1. INTRODUCTION

Thanks to several successful projects worldwide, several countries have been developing design recommendations and codes for Ultra-High Fibre Reinforced Performance Concrete (UHPFRC) [1]–[4]. Exceptionally, UHPFRC design principles account for the tensile behaviour, which is key for assuring limited crack widths for durability concerns. The non-linear tensile law of UHPC is threefold: (i) a linear elastic part up to the first crack of the cementitious matrix; (ii) a strain-hardening part which is associated with the formation of multiple microcracks bridged by uniformly distributed short steel microfibers; (iii) a final softening part which is associated with the crack opening of a major crack.

Uniaxial Tensile Test (UTT) is evidently the most *direct* method to characterize the UHPFRC tensile law [5]. However, this kind of test has 3 major drawbacks: (i) sophisticated closed-loop systems which are required to control the test are not always available in common laboratory [6]; (ii) the test results are significantly affected by the boundary conditions (e.g., press platen stiffness) and loading alignment [7]–[10]; (iii) cracks often can grow asymmetrically and sometimes create complex branching [11].

Therefore, the identification of the UHPFRC tensile constitutive law from a bending test has been the focus of several recommendations. The results of a bending tests on UHPFRC are usually analysed by inverse analysis to estimate the tensile law. A comprehensive introduction to the inverse analysis method can be found in Chanvillard et al. [12], and Casanova & Rossi [13]. The determination of the Moment-Curvature (M-X) from the tensile law mathematically consists in solving four equations with 4 unknowns (maximum curvature χ, neutral axis position α_n*h, crack height α*h, tensile stress σ_t at the crack mouth opening w_0). In details, the governing equations are: 2 equations from mechanical equilibrium of the section (moment and axial force) of the plain section with a non-linear tensile law, a relationship between the tensile strength and the curvature, and compatibility relation between the rotation of the beam across the characteristic length of the plastic hinge (see Figure 2a). By an iterative method, this procedure can be numerically inverted [12]. As for numerical issues, a data fitting algorithm iterative method has been developed to bypass the issue of non-uniqueness of solution of such inverse analysis [14], [15]. The inverse analysis requires the measurement of the crack mouth opening (w_0), or equivalently, of the mid-span deflection, which can be estimated by integrating the curvature distribution. Once the crack has localized, the beam behaves as a hinge mechanism between 2 rigid parts, that is, the relationship between deflection and crack mouth opening is mostly linear.

By the use of the concept of characteristic length L_{ch}, which transforms the crack opening into an equivalent strain, the method can be simplified as it reduces to analysis of a cracked section with nonlinear tensile law [13]. Unfortunately, the definition of L_{ch} which can be found in open literature can vary considerably, from h/2 to 2h (where h is the section height), as explained in a recent review on the subject [16].

From a theoretical perspective, Chanvillard proved that it is possible to obtain flexural hardening behaviour with a tensile law with a post-peak strength of 50% of the maximum strength. That means, deflection-hardening in bending does not mean strain-hardening in tension. From an experimental side, Baby et al. showed that the flexural hardening behaviour of UHPFRC may be characterized by two distinguished multiple crack distribution: cluster distribution of micro-cracks (also called multiple macrocrack) and uniformly distributed microcracks [17]. Interestingly, an inverse analysis method was then developed in order to distinguish between UHPFRC with strain-hardening stress-strain hardening law up to the peak load, followed by a stress-crack opening law from UHPFRC with only the latter behaviour [18].

More generally, the estimation of the tensile law from inverse analysis can depend on simplified assumptions related to the beam deformation kinetics, such as, the multiple microcrack distribution, the elastic unloading after localization (which relates to the capacity of micro-cracks to re-close), the distribution of the curvature nearby the localized crack, and location of the major crack. This work aims at developing a method with less assumptions on the micro-crack distribution and location of the major crack for estimating the UHPFRC tensile constitutive law from a bending test, by means of Digital Image Correlation (DIC).

2. MATERIALS AND METHOD

2.1 Specimens

We employed a UHPFRC material (under the commercial name of Ductal® G2 FM) composed by 2200 kg/m^3 of premix mixture of hydraulic cementitious constituents and inert materials, 30 kg/m^3 of high-range water-reducing admixture, 130 kg/m^3 of water and steel fibres with a volume content V_f of 1 % or 2 %. The steel fibres have a length of 14 mm and diameter of 0.185 mm with an aspect ratio (L/d) of 75, a Young's modulus of about 200 GPa and a yielding stress of 2860 MPa. For each beam geometry (short and long beams), 2 different series of 4 beams were tested, such as: (1) UHPFRC with a fiber volume content V_f = 1 %; (2) UHPFRC with V_f = 2 %. Two series of 4 beams were cast by varying the fibre volume content (V_f = 1 or 2 %). Each beam had a width of about 40 mm, a height of 100 mm, a span of 1200 mm, a length of 1400 mm, and a load span of 400 mm as shown in Figure 1.The choice of dimension was made to check possible shear and size effects.

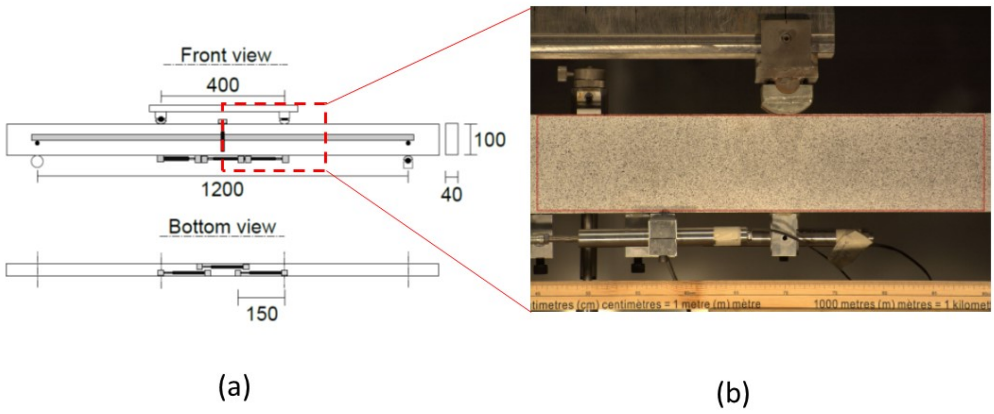

Figure 1. (a) test set-up for 4PBT with LVDT positions; (b) example of surface preparation of the bottom beam surface for image analysis.

2.2 Test methods

The following laboratory tests were carried out: (1) flow-table tests; (2) compressive strength test; (3) chloride migration test; (4) grinding test and (5) chloride titration. As for the Digital Image Correlation (DIC), considering the Euler Bernoulli beam kinetics with a varying position of the neutral axis which accounts for damage process zone [19]. Once the beam deflection and rotation have been estimated by inverse analysis, the UHPFRC moment-curvature relationship was estimated by best fitting the beam deflection and rotation measured by DIC analysis along the entire beam at all time steps. In order to account the crack discontinuity, which occurs approximately at the peak load, a rotation jump function was also assumed and estimated by the best fitting procedure.

Following the approach of Chanvillard [12], Figure 2a shows the mechanisms of rotation compatibility employed in this work for which

$$\theta = \int_0^{L_{ch}/2} \chi(x)dx = \frac{w_0}{2\alpha h} \tag{1}$$

Figure 2b shows the measured rotation (θ) profile along the beam in the proximity of the localized crack by means of DIC analysis. The experimental profile is compared with the idealized one with parabolic distribution of curvature proposed by Chanvillard [12] and constant curvature with a jump of rotation.

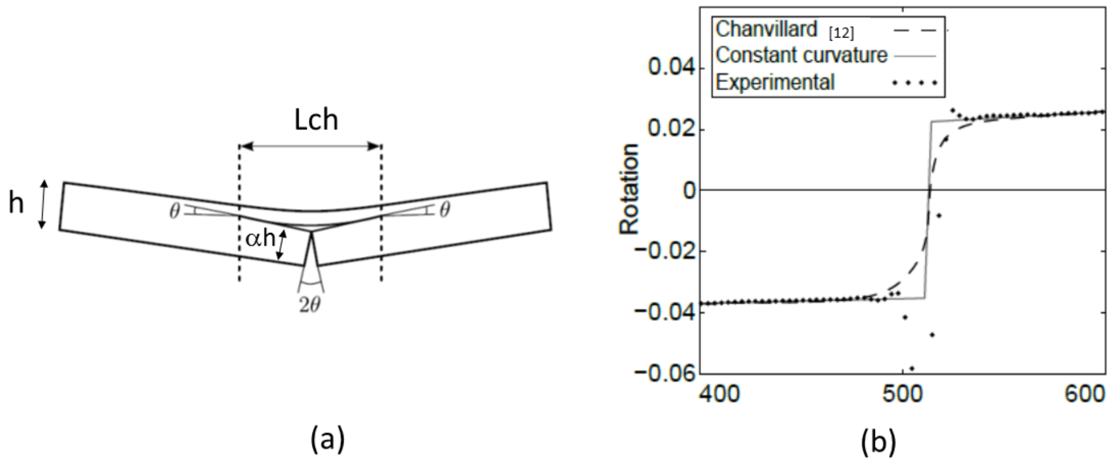

Figure 2. (a) mechanism of rotation compatibility;
(b) comparison between the experimental rotation measured by DIC analysis across the characteristic length L_{ch} zone with idealized curvature distribution (constant and parabolic).

Operatively, the present method is decomposed in three steps: (i) use of DIC analysis to identify both M-X relationship (before crack localization) and M-θ afterwards; (ii) use of DIC analysis to estimate the characteristic length L_{ch} by solving Eq.(1) and estimation of the equivalent M-X relationship which homogenizes the localized crack (Figure 2b) by means of the estimated L_{ch}; (iii) identification of the tensile law which best fits the M-X relationship by least-squares methods. This last step is carried out by considering recently developed relations which explicitly link the tensile law in terms of stress-strain σ-ε to the position of the neutral axis and the total moment [20].

3. RESULTS

Figure 3a and 3b show the load vs. deflection of the series samples for the volume fraction of 1 % and 2 %, respectively. The test repeatability is rather satisfactory as the major difference comes from the position of the point of the bifurcation at which the loading softening curve starts, which depends on the position and time of the localization of the major crack. Both material showed flexural hardening, although the hardening load-displacement branch is more pronounced for the V_f = 2 %.

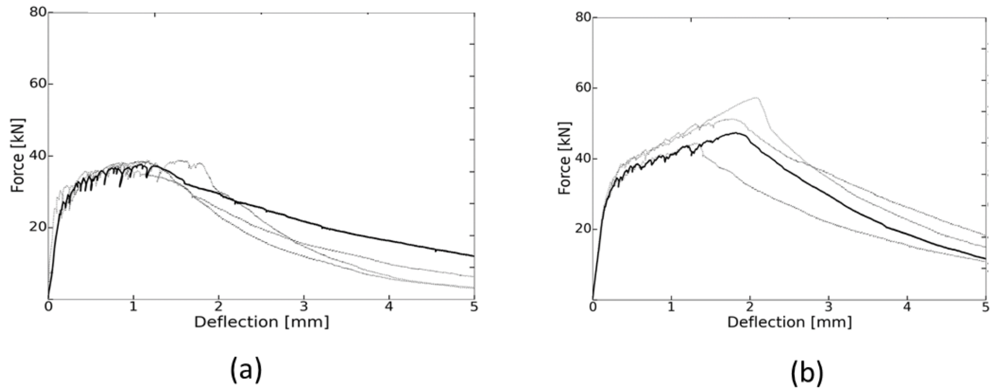

Figure 3. Load vs. deflection curves for UHPFRC with (a) V_f = 1 % and (b) V_f = 2 %.

Table 1shows the typical multiple crack pattern observed for the two UHPFRC at V_f = 1 % and V_f = 2 %. Interestingly, for the case with V_f = 1 %, the multiple cracks are not uniformly spaced, but the microcracks form in a microcrack cluster spaced of about 45 mm (other work called this pattern as “multiple macro-cracks” [17]). The beam with V_f = 2 % showed multiple micro-cracks uniformly spaced at the distance which is close to the fibre length. Table 1 also reports the mean value and standard deviation of the micro-crack number and their spacing.

Table 1. Crack statistics as observed by naked eye for V_f = 1 % and V_f = 2 %

V_f [%]	Number of cracks	Microcrack spacing [mm]	Microcrack Pattern	Photo
1	25 ± 8	45 ± 5	Clusters	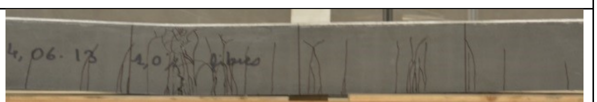
2	90 ± 16	9 ± 2	Uniform	

As for the DIC analysis, Figure 4 shows the comparison between measured (points) and DIC simulated (continuous curve) for the deflection and slope of the beam at different time. The fitting of the deflection is rather excellent along the entire beam at all time, while the rotation is also well captured with exception within the characteristic zone L_{ch} close to the rotation discontinuity (localized crack). Therefore, the proposed method accounts for the non-uniform micro-cracking distribution and the possible non-symmetric position of the localized crack in the estimation of the sectional moment-curvature relationship and the plastic length.

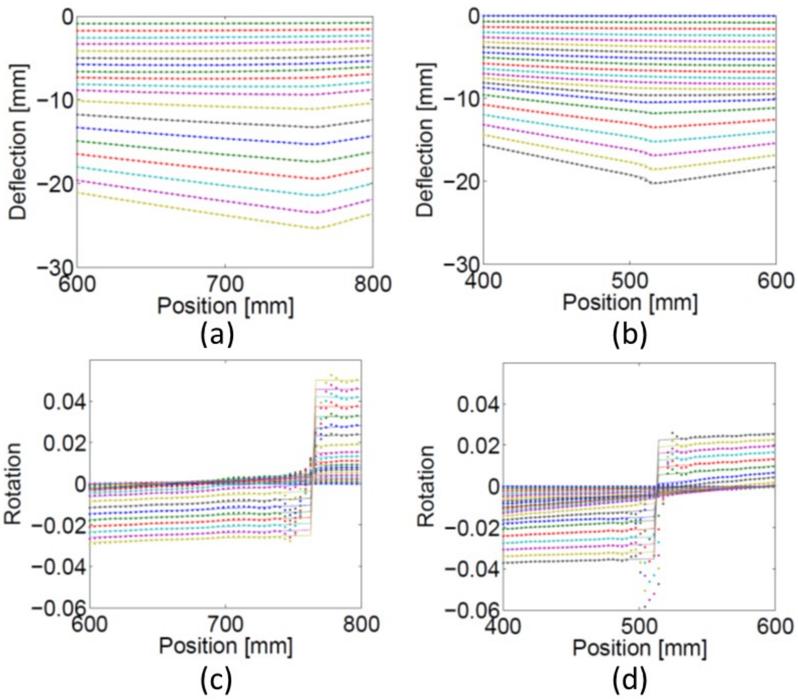

Figure 4. Comparison between the experiments (points) and the simulation (continuous line) for the deflection and slope of beams (a, c) $V_f = 1$ % and (b, d) $V_f = 2$ % at different time.

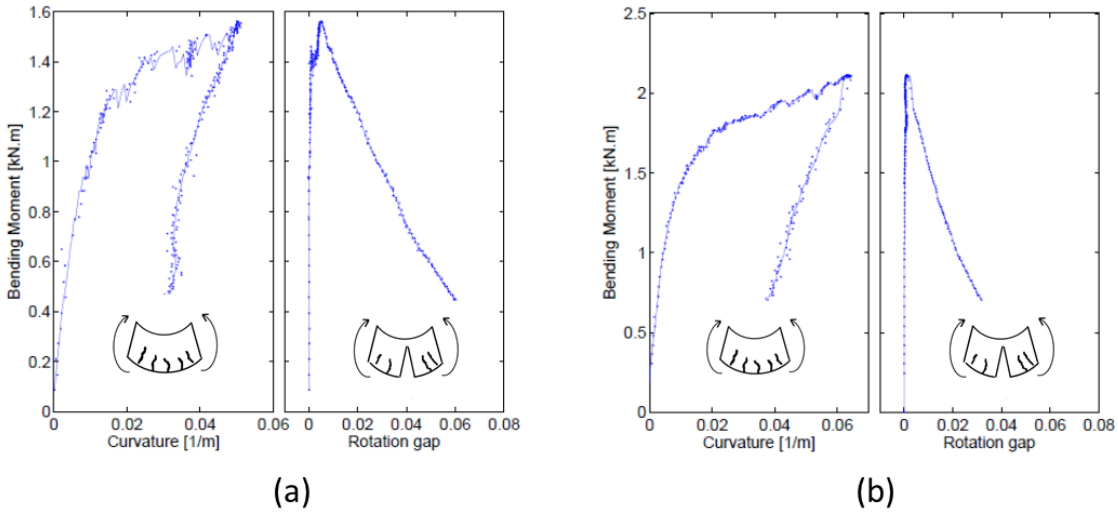

Figure 5. DIC analysis results for the reference beam with Vf = 1% in term of moment-curvature (a-1) and moment rotation (a-2). Analogously, for the reference beam with Vf = 2% in term of moment-curvature (b-1) and moment rotation (b-2).

Figure 5a and 5b show the best fitting of the moment-curvature M-X relationship (up to the peak load) and moment-rotation M-θ for $V_f = 1$ % and $V_f = 2$ %, respectively. Notably, the result accounts for elastic unloading of the microcracks (the linear unloading of the M-X curvature relationship). Finally, the proposed method allows also identifying the exact crack localization which occurs slightly before the peak by considering the load level of the P-θ relationship [21].

Figure 6 shows the L_{ch} which satisfy the Eq.(1) of the mechanisms of rotation compatibility [12] as evaluated by DIC analysis. Interestingly, for $V_f = 1$ %, L_{ch} varies from about 50 mm to 175 mm, which is close to 7/4 x h (Figure 6a). That is, the damage process is governed first by the fibre bridging mechanisms and the micro-cracks' spacing, while later is governed by the structural behaviour of the cracked beam. As for $V_f = 2$ %, Figure 6b shows that the initial L_{ch} is slightly less and close to 35-40 mm.

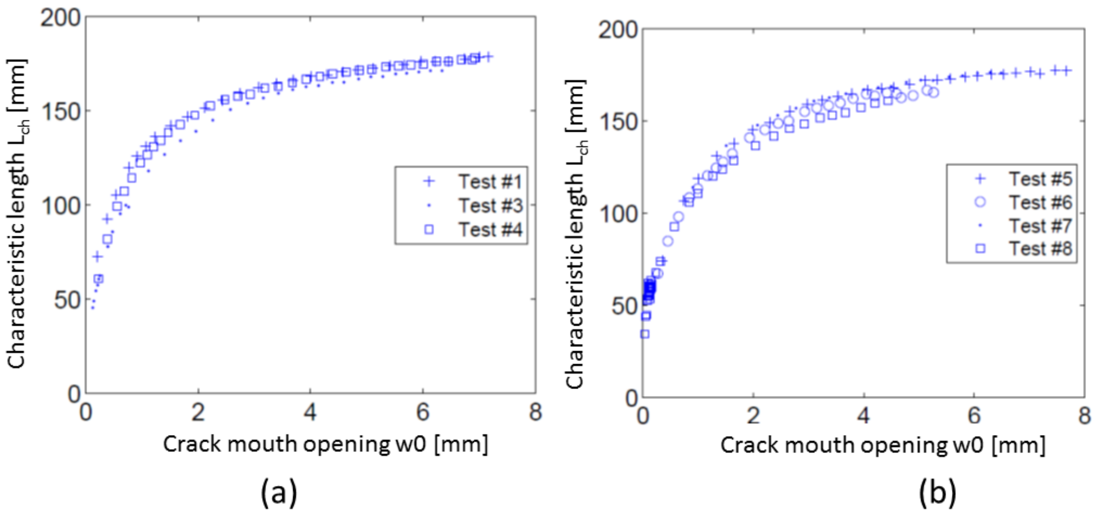

Figure 6. Characteristic length identified by DIC analysis for (a) V_f= 1 % and (b) V_f= 2 %.

Figure 7 shows the M-X relations estimated by simply converting the post-peak M-θ relationships (Figure 5) into an equivalent M-X relationship by means of the estimated L_{ch} (Figure 6).

Finally, the UHPFRC tensile constitutive law can be derived by the M-X relationship. The elastic limit of 12.6 MPa can be easily identified by the end of linearity of the load-deflection curve by DIC analysis. The rest of the tensile law σ-ε is then estimated by best-fitting the M-X relationships (Figure 7) by means of the explicit relationships between σ-ε, the neutral axis position and the moment [20]. After the maximum stress, the strain can be converted in equivalent crack opening as L_{ch}. Figure 8 compares the so-obtained tensile law for V_f= 1 % and V_f= 2 % with the present method and with the one proposed by Baby et al. [18]. Interestingly, the proposed DIC based method predicted a softening law (i.e., post-cracking strength lower than the elastic limit) for V_f= 1 %, and a strain hardening law for V_f= 2 %. The comparison with existing method is also satisfactory.

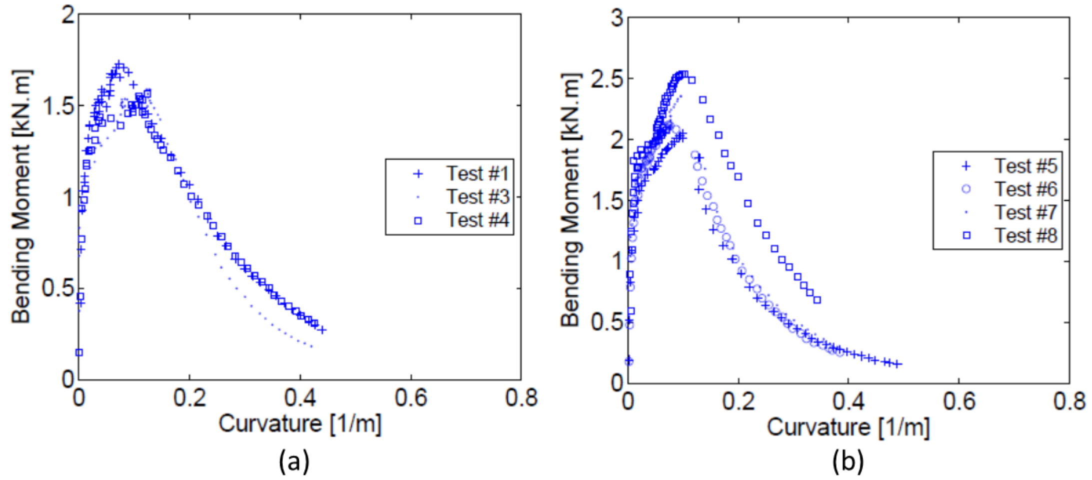

Figure 7. Continuum moment-curvature relationship identified by DIC analysis for (a) $V_f = 1$ % and (b) $V_f = 2$ %.

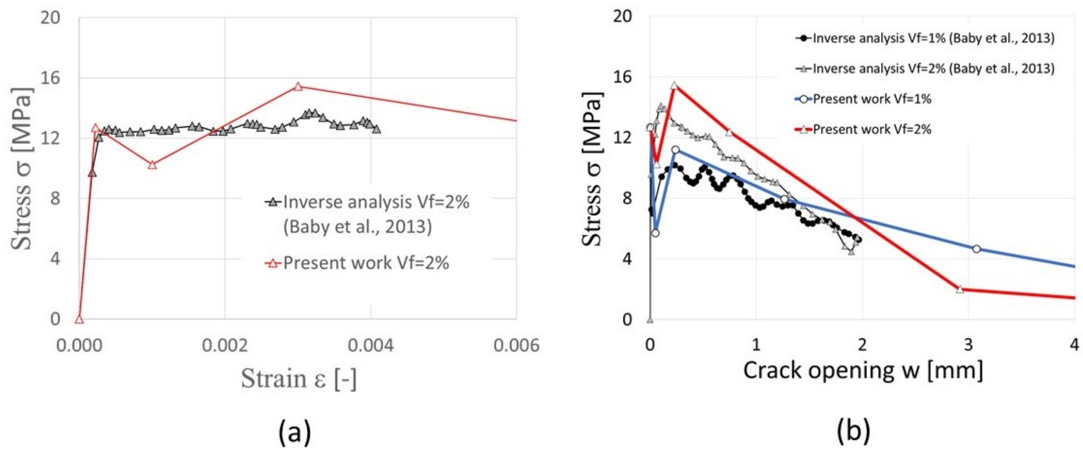

Figure 8. Comparison between the inverse analysis method and the present DIC method for (a) stress-strain law of $V_f = 2$ % and (b) stress-crack opening law for $V_f = 1$ % and $V_f = 2$ %.

4. CONCLUSIONS

This article investigates a new method based on Digital Image Correlation (DIC) to assess the moment-curvature of a UHPFRC by filtering structural effects, such as, the distribution of the multiple cracks, the position of the localized crack, and the elastic unloading. Based on the present results, the following conclusions can be drawn on the proposed DIC based inverse analysis:

1. The first cracking strength can be identified with accuracy from the end of linearity of the load-deflection curve of unnotched beams;
2. The moment-curvature M-X as well as the moment-rotation M-θ can be identified in a physical sound manner with information on the micro-crack unloading and the exact load of the crack localization (which is slightly before the peak load);
3. The characteristic length L_{ch} is identified varying from a size which is comparable to the fibre length (4 times) to a final size which is a fraction of the beam height (7/4);
4. Once the M-X is estimated, explicit formula can be employed to back-analyse the stress-strain σ-ε tensile law of UHPFRC;
5. The method is able to automatically distinguish softening from strain-hardening

The present method can be easily implemented in software as an automatic procedure to estimate UHPFRC tensile law from bending. Further validation is on-going by considering different beam geometry and the combined use of steel reinforcement.

ACKNOWLEDGEMENT

The Authors would like to thank Mr Vernet for the careful preparation of the UHPFRC samples. Furthermore, a special thanks to the memory of Mr. Gilles Chanvillard†, who has much inspired this work with precious advices.

REFERENCES

[1] Japan Society of Civil Engineers JSCE, 'Recommendations for Design and Construction of High Performance Fiber Reinforced Cement Composites with Multiple Fine Cracks (HPFRCC)', 2008.

[2] AFGC/SETRA, 'Ultra-high performance fibre-reinforced concretes - Recommendations', *Interim Recomm. AFGC Publ. Fr.*, 2013.

[3] SIA 2052, 'Béton fibré ultra-performant (UHFB) – Matériaux, dimensionnement et exécution. Projet final après mise en consultation', Cahier technique, 2014.

[4] AFNOR, 'Complément national à l'Eurocode 2 : calcul des structures en béton - règles spécifiques pour les BFUP', 2016.

[5] B. Graybeal and F. Baby, 'Development of Direct Tension Test Method for Ultra-High-Performance Fiber-Reinforced Concrete', *ACI Mater. J.*, vol. 110, no. 2, pp. 177–186, 2013.

[6] J. G. M. Van Mier and C. Shi, 'Stability issues in uniaxial tensile tests on brittle disordered materials', *Int. J. Solids Struct.*, vol. 39, no. 13, pp. 3359–3372, 2002.

[7] S. Cattaneo and G. Rosati, 'Effect of different boundary conditions in direct tensile tests: experimental results', *Mag. Concr. Res.*, vol. 51, no. 5, pp. 365–374, 1999.

[8] J. G. M. Van Mier and M. R. A. Van Vliet, 'Uniaxial tension test for the determination of fracture parameters of concrete: state of the art', *Eng. Fract. Mech.*, vol. 69, no. 2, pp. 235–247, 2002.

[9] L. G. Sorelli, A. Meda, and G. A. Plizzari, 'Bending and uniaxial tensile tests on concrete reinforced with hybrid steel fibers', *J. Mater. Civ. Eng.*, vol. 17, no. 5, pp. 519–527, 2005.

[10] J. G. M. Van Mier and A. Vervuurt, 'Micromechanical analysis and experimental verification of boundary rotation effects in uniaxial tension tests on concrete', *Fract. Brittle Disord. Mater. Concr. Rock Ceram. Lond. E FN Spoon*, pp. 406–20, 1995.

[11] Z. P. Bažant and L. Cedolin, 'Why direct tension test specimens break flexing to the side', *J. Struct. Eng.*, vol. 119, no. 4, pp. 1101–1113, 1993.

[12] G. Chanvillard, 'Characterisation of fibre reinforced concrete mechanical properties: a review', *Fiber-Reinf. Concr. BEFIB'2000 RILEM Proc. PRO15*, pp. 29–49, 2000.

[13] P. Casanova and P. Rossi, 'Analysis and design of steel fiber reinforced concrete beams', *ACI Struct. J.*, vol. 94, no. 5, pp. 595–602, 1997.

[14] A. Nour, B. Massicotte, R. de Montaignac, and J.-P. Charron, 'Development of an inverse analysis procedure for the characterisation of softening diagrams for FRC beams and panels', *Constr. Build. Mater.*, vol. 94, pp. 35–44, 2015.

[15] A. M. Alvaredo and R. J. Torrent, 'The effect of the shape of the strain-softening diagram on the bearing capacity of concrete beams', *Mater. Struct.*, vol. 20, no. 6, pp. 448–454, 1987.

[16] R. de Montaignac, B. Massicotte, and J.-P. Charron, 'Design of SFRC structural elements: flexural behaviour prediction', *Mater. Struct.*, vol. 45, no. 4, pp. 623–636, 2012.

[17] F. Baby, B. A. Graybeal, P. Marchand, and F. Toutlemonde, 'Identification of UHPFRC tensile behaviour: methodology based on bending tests', in *UHPFRC 2013-International Symposium on Ultra-High Performance Fibre-Reinforced Concrete*, 2013, pp. 649 – 658.

[18] F. Baby, B. Graybeal, P. Marchand, and F. Toutlemonde, 'UHPFRC tensile behavior characterization: inverse analysis of four-point bending test results', *Mater. Struct.*, vol. 46, no. 8, pp. 1337–1354, 2013.

[19] P. Leplay, J. Réthoré, S. Meille, and M.-C. Baietto, 'Damage law identification of a quasi brittle ceramic from a bending test using Digital Image Correlation', *J. Eur. Ceram. Soc.*, vol. 30, no. 13, pp. 2715–2725, 2010.

[20] G. Chanvillard and D. Corvez, 'Explicit back analysis method for quick determination of direct tensile strength of plate structural members', in *RILEM-fib-AFGC Int. Symposium on Ultra-High Performance Fibre-Reinforced Concrete, UHPFRC 2013*, 2013, pp. 659 – 668.

[21] A. Spasojevic, D. Redaelli, M. Fernández Ruiz, and A. Muttoni, 'Influence of tensile properties of UHPFRC on size effect in bending', in *Ultra High Performance Concrete (UHPC), Second International Symposium on Ultra High Performance Concrete*, 2008, pp. 303–310.